

Crystallization of rapidly quenched ribbons on the base of $\text{Fe}_{82}\text{Si}_2\text{B}_{16}$ under isothermal annealing

O.P.Brud'ko, V.K.Nosenko , M.I.Zakharenko, Yu.P.Skljarov*

Department of Physics, T.Shevchenko Kyiv University,
64 Volodymyrska St., 01033 Kyiv, Ukraine

*G.Kurdyumov Institute for Metal Physics, National Academy of Sciences
of Ukraine, 36 Vernadsky Ave., 04680 Kyiv, Ukraine

The crystallization kinetics of the amorphous alloys on the base of $\text{Fe}_{82}\text{Si}_2\text{B}_{16}$ has been studied under isothermal annealing using magnetometric method. The apparent crystallization activation energy of E_a and Avrami exponent n have been determined. The admixtures of Ni and Mo have been shown to influence weakly on the values of E_a and n . The apparent activation energy of crystallization for the ribbons produced using industrial raw materials coincides within the experiment accuracy with that for the alloys of identical composition produced from chemically pure components. It has been also ascertained that the n value is determined mainly by the chemical composition of alloy rather than by the thickness of the rapidly quenched ribbon.

Магнитометрическим методом исследована кинетика кристаллизации аморфных сплавов на основе $\text{Fe}_{82}\text{Si}_2\text{B}_{16}$ в процессе их изотермических отжигов. Определены энергия активации кристаллизации E_a и показатель Аврама n . Показано, что добавки Ni и Mo слабо влияют на значения E_a и n . Энергия активации кристаллизации для лент, изготовленных с использованием промышленных лигатур, в пределах погрешности совпадает с соответствующим значением для сплавов того же состава, изготовленных из химически чистых компонентов. Установлено также, что величина n зависит, главным образом, от состава аморфного сплава, а не от толщины быстрозакаленной ленты.

Amorphous metallic alloys (AMAs) on the base of Fe–Si–B system are suitable as core materials in distribution transformers because of their low core losses and relatively high saturation magnetization. These properties are improved or at least remain unchanged when doping the alloys of the above basic composition with Ni and Mo. It has been established that complex doping of the basic AMA composition with Ni and Mo increases the resistivity thereof from 90–120 to 130–160 $\mu\Omega\cdot\text{cm}$, thus favoring to reduce the eddy currents energy losses [1] and essentially influences crystallization temperature T_x and the majority of magnetic parameters [2]. Optimum proportions of these dopants enable to provide desirable combination of service characteristics.

On the other hand, the doping elements may strongly affect the thermal stability under real operational conditions. Therefore, the crystallization of the alloys has been extensively studied. Although a number of works have reported the crystallization process of Fe–Si–B AMAs [3–5], there are very few studies on its relation to the amorphous structure and the presence of 3d admixtures. The crystallization behavior of some AMAs including Fe–Si–B alloys has been examined by transmission electron microscopy, X-ray diffraction and differential thermal analysis, and a general transformation sequence on crystallization of the AMAs has been proposed. The crystallization kinetics in hypoeutectic, eutectic and hypereutectic Fe–Si–B AMAs has been studied in [4] and the compositional depend-

Table. Apparent activation energy of crystallization (E_a) and Avrami exponent (n) for AMAs on the base of $\text{Fe}_{82}\text{Si}_2\text{B}_{16}$

#	Content	Type of AMA	Thickness D , μm	E_a , kJ/mole	n
1	$\text{Fe}_{82}\text{Si}_2\text{B}_{16}$	<i>c</i>	30	340	2.7
2	$\text{Fe}_{75.5}\text{Si}_2\text{B}_{16}\text{Ni}_{3.5}\text{Mo}_3$	<i>c</i>	28	280	2.4
3	$\text{Fe}_{75.5}\text{Si}_2\text{B}_{16}\text{Ni}_{3.5}\text{Mo}_3$	<i>t</i>	40	220	2.8
4	$\text{Fe}_{75.5}\text{Si}_2\text{B}_{16}\text{Ni}_{3.5}\text{Mo}_3$	<i>t</i>	28	280	2.8
5	$\text{Fe}_{75.5}\text{Si}_2\text{B}_{16}\text{Ni}_{3.5}\text{Mo}_3$	<i>t</i>	30	250	2.8
6	$\text{Fe}_{75.5}\text{Si}_2\text{B}_{16}\text{Ni}_{3.5}\text{Mo}_3$	<i>t</i>	30	290	2.7
7	$\text{Fe}_{78}\text{Si}_2\text{B}_{16}\text{Ni}_1\text{Mo}_3$	<i>c</i>	28	240	2.9
8	$\text{Fe}_{77.5}\text{Si}_2\text{B}_{16}\text{Ni}_{3.5}\text{Mo}_1$	<i>c</i>	32	300	2.9

ence of the effective crystallization activation energy and the Avrami exponent have been reported. Although the compositional dependence of the Fe–Si–B AMAs crystallization process has been extensively examined from the various points of view as mentioned above, very few studies have been reported on the relation of the crystallization behavior to amorphous structure. Recently, a structural model that explains well the compositional dependence of structure-sensitive properties and crystallization kinetics of Fe–Si–B AMAs has been proposed [5]. The purpose of this work is to investigate the influence of Ni and Mo dopants on $\text{Fe}_{82}\text{Si}_2\text{B}_{16}$ crystallization kinetics and to examine the possibilities to use the industrial raw materials for AMAs processing.

Amorphous metallic alloys on the base of $\text{Fe}_{82}\text{Si}_2\text{B}_{16}$ shaped as 10 mm wide and 20–40 μm thick ribbons have been prepared by single-roll quenching technique. The samples were prepared both from chemically pure components (*c*-glasses) and from industrial raw materials (*t*-glasses). The *t*-glasses have been produced using the industrial FB-17 Fe–B alloy (containing up to 20 mass % B, 1.4 mass % Al, 0.4 mass % Si, 0.1 mass % C), raw silicon (99.4 mass % purity), Mo and Ni (99.8 mass % purity). The *c*-glasses have been produced using Fe (99.96 mass %), Ni (99.92 mass %), Mo (99.9 mass %), semiconducting Si (99.999 mass %) and amorphous B (99.9 mass %). The melt temperature before ejecting through rectangular nozzle was 1300–1350°C, the speed of a disk made of chromic bronze 600 mm in diameter was 820–850 min^{-1} . The melt ejecting pressure of the changed within limits of 15–25 kPa. The gap between nozzle and disk was increased from 0.15–0.2 mm

up to 0.25–0.3 mm. The AMA contents have been controlled by the X-ray fluorescence and are presented in the Table.

Magnetometric measurements have been used to analyze the crystallization kinetics, because the crystallization of Fe–Si–B AMAs is accompanied by a sharp rise of magnetization due to formation of crystalline phases with elevated Curie points. Magnetometric investigations were carried out using a Faraday type magnetometer with microbalance in the temperature range 300–850 K in the purified argon atmosphere. The accuracy of the susceptibility measurements $\Delta\chi/\chi$ was better than 1.5 % and that of temperature $\Delta T \leq 0.5$ K. Prior to performing magnetometric measurements, all samples were analyzed by X-ray diffraction. The results provide an evidence for the amorphous structure of all as-quenched ribbons. No crystalline inclusions were detected.

Temperature dependences of magnetic susceptibility $\chi(T)$ have been studied in details in [2]. The crystallization of all studied AMAs was found to occur through a single stage that is typical of eutectic and hypereutectic alloys [6] and to be accompanied by an essential rise of χ . This is seen clearly in Fig. 1 which presents $\chi(T)$ curve for $\text{Fe}_{82}\text{Si}_2\text{B}_{16}$ glass as an example, and evidences the simultaneous formation of Fe_3B and $\alpha\text{-Fe}$ based solid solution. A substantial increase of χ upon crystallization of the investigated AMAs promoted the application of magnetometric method to the analysis of its kinetics. Crystallization of amorphous alloys is well described by the phenomenological Avrami equation:

$$x = (1 - at^n), \quad (1)$$

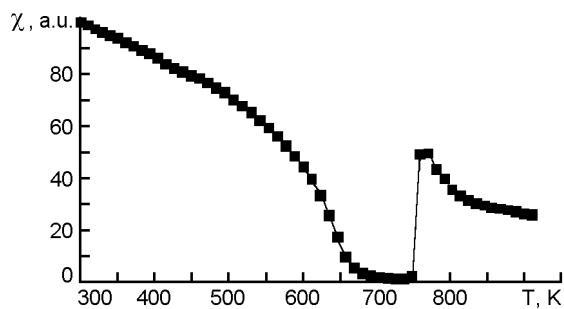


Fig. 1. Temperature dependence of magnetic susceptibility for as-prepared $\text{Fe}_{82}\text{Si}_2\text{B}_{16}$ AMA.

where x is the crystalline fraction at the time t , a and n are known as the rate parameter and Avrami exponent, respectively [7]. Since we analyze the crystallization kinetics proceeding from the data on magnetic susceptibility, it is advisable to present Eq.(1) as

$$\frac{\chi_k - \chi(t)}{\chi_k - \chi_a} = \exp(-at^n), \quad (2)$$

or in an equivalent form:

$$\text{lg} \lg \frac{\chi_k - \chi_a}{\chi_k - \chi(t)} = \text{lg} a + n \text{lg} t \quad (3)$$

through a sequence of routine transformations. Here, χ_a and χ_k are the susceptibilities of the as-prepared and totally crystallized material, $\chi(t)$ is the susceptibility at the time t . So, in order to analyze the crystallization kinetics using magnetometric method, it is necessary to obtain the dependences of χ vs. time t of isothermal annealing at different temperatures close to the crystallization temperature T_x . The annealing temperature values for each studied AMA were selected basing on the appropriate data on T_x listed in [2]. The procedure of such analysis is presented in detail in [8]. Fig. 2 presents typical sets of $\chi(t)$ curves fitted according to Eq.(3). Evidently, each $\chi(t)$ curve exhibits a linear region that confirms the validity of the Avrami equation. This allows to determine n and the transformation time. The n values obtained are found to decrease slightly at higher annealing temperatures. As it is clearly seen from Fig. 3, the transformation time is governed by the Arrhenius law:

$$t = t_0 \exp[E_a/kT], \quad (4)$$

where T is the temperature; k , the Boltzmann constant; E_a , the apparent activation energy of crystallization and t_0 , a time constant. The values of E_a and n derived from the experimental data are summarized in the Table (the estimated errors are ± 20 kJ/mole in E_a and ± 0.2 in n).

The obtained E_a and n values for the basic $\text{Fe}_{82}\text{Si}_2\text{B}_{16}$ AMA is in a fairly good agreement with the data of [4]. However, it should be noted that the presence of both Mo and Ni results in a decrease of E_a , the influence of Mo being considered to be of more significance. The presence of Ni in Fe-Si-B AMAs for high-frequency applications is necessary from the standpoint of their magnetic properties [9]. Another important result is the fact that the crystal-

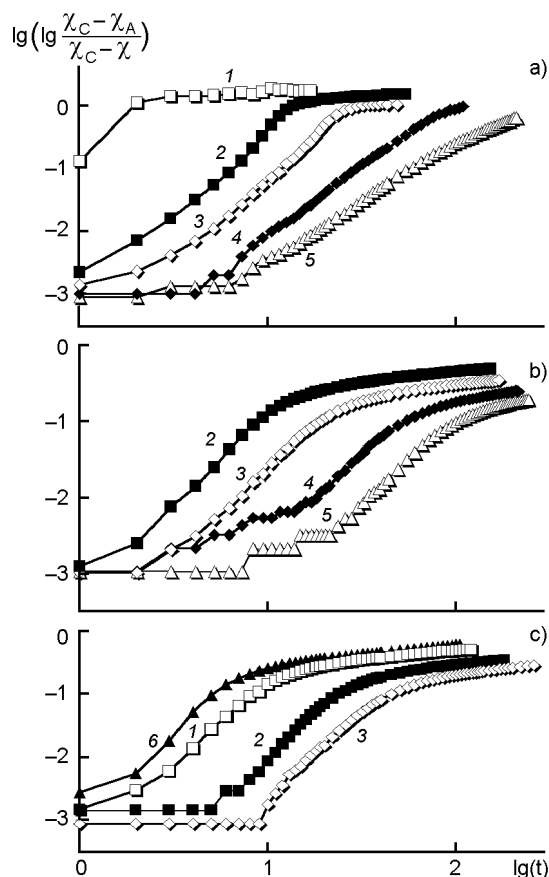


Fig. 2. Dependences of $\text{lg} \lg \frac{\chi_k - \chi_a}{\chi_k - \chi(t)}$ vs. $\text{lg} t$ for $\text{Fe}_{82}\text{Si}_2\text{B}_{16}$ (c-glass) (a), $\text{Fe}_{78}\text{Si}_2\text{B}_{16}\text{Ni}_1\text{Mo}_3$ (c-glass) (b) and $\text{Fe}_{75.5}\text{Si}_2\text{B}_{16}\text{Ni}_{3.5}\text{Mo}_3$ (t-glass) (c) obtained at $T = 660$ (5), 670 (4), 680 (3), 690 (2), 700 (1) and 710 K (6).

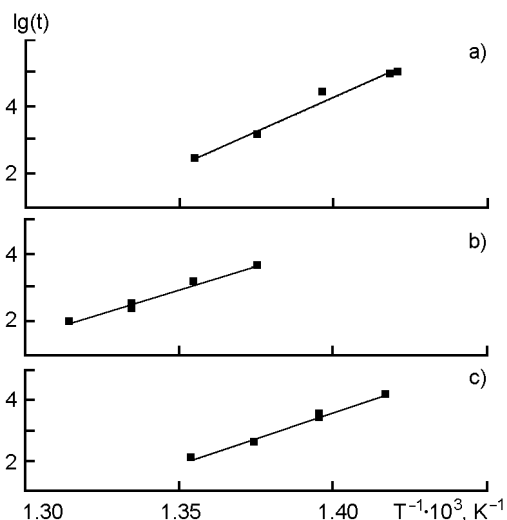


Fig. 3. Dependences of $\lg t$ vs. T^{-1} for $\text{Fe}_{82}\text{Si}_2\text{B}_{16}$ (*c*-glass) (a), $\text{Fe}_{78}\text{Si}_2\text{B}_{16}\text{Ni}_1\text{Mo}_3$ (*c*-glass) (b) and $\text{Fe}_{75.5}\text{Si}_2\text{B}_{16}\text{Ni}_{3.5}\text{Mo}_3$ (*t*-glass) (c).

lization activation apparent energy occurred to be almost the same for *c*- and *t*-glasses of identical composition (within the experiment accuracy) that provides the possibility to use industrial raw materials in AMAs' processing. However, the values of E_a exhibit a trend to decrease with increasing ribbon thickness. This may reflect the influence of atomic inhomogeneities being formed in Fe–Si–B AMAs doped by Ni and Mo [2].

The Avrami exponent n , according to [7], could be factorized as follows:

$$n = n_1 + n_2 \cdot p. \quad (5)$$

Here n_1 is determined by the nucleation rate and varies from 0 (for quenched-in nuclei) to 1 (for constant nucleation rate), n_2 takes a value of 1, 2 or 3 depending on the dimensionality of the crystal growth. The parameter p is determined by the mechanism that controls crystal growth and is equal either to 0.5 for diffusion controlled (parabolic) growth or to 1 for interfacial (linear in time) growth. Since the crystallization process in Fe–B AMAs is known to be diffusion-controlled [10], one can expect n being equal to 2.5 in the case of linear nucleation rate. However, $n > 2.5$ for all investigated alloys (except for AMA #2).

Reasoning from the findings presented in [4], according to which the nucleation rate in this type of AMA is suppressed by the presence of Si, we consider this fact as the evidence that due to addition of Si, the crystal growth becomes not purely diffu-

sion-controlled (i.e. $0.5 < p < 1$). Another important observation is that the *t*-glasses are characterized by somewhat higher n values than *c*-glasses of similar composition. We believe that the only reason of such behavior is that p in a former case is higher, closer to 1. This is confirmed by the data of direct determination of p by transmission electron microscopy [11]. In contrast to E_a , no effect of ribbon thickness on the n values is found, thus allowing to conclude that the processes of nucleation and growth are determined mainly by the chemical composition of AMA rather than by solidification parameters. The slight increase of n with increasing annealing temperature, as mentioned above, has been also observed for other amorphous systems [12]. According to [4], this may be attributed to some increase of n_1 , though the physical nature of this phenomenon remains obscured.

Thus, the apparent activation energy of crystallization E_a is weakly influenced by Ni and Mo additions to $\text{Fe}_{82}\text{Si}_2\text{B}_{16}$ and is almost the same for *c*- and *t*-glasses of identical composition (though the E_a values exhibit a trend to decrease with increasing ribbon thickness). This supports the statement that the industrial raw materials are of good prospects to use for Fe–Si–B AMAs manufacturing due to lower process costs. Values of the Avrami exponent n suggest that the crystallization of the studied AMAs is not purely diffusion-controlled (it is intermediate between parabolic and linear growth) and is determined mainly by the chemical composition of AMA rather than by solidification parameters.

References

1. V.V.Maslov, V.K.Nosenko, *J. Met. Phys. and Adv. Technol.*, **16**, 5 (1994).
2. V.Maslov, O.Nakonechna, V.Nosenko et al., *Functional Materials*, **7**, 822 (2000).
3. D.S.dos Santos, D.R.dos Santos, *J. Non-Cryst. Solids*, **304**, 56 (2002).
4. V.R.V.Ramanan, G.E.Fish, *J. Appl. Phys.*, **53**, 2273 (1982).
5. J.M.Dubois, G.Le Caer, *Acta Metall.*, **32**, 2101 (1984).
6. J.C.Swartz, R.Kossovsky, J.J.Haugh et al., *J. Appl. Phys.*, **52**, 3324 (1981).
7. J.W.Christian, *The Theory of Transformation in Metals and Alloys*, Pergamon Press, New York (1975).
8. A.P.Shpak, Yu.A.Kunitskiy, M.I.Zakharenko, A.S.Voloshchenko, *Magnetism of Amorphous and Nanocrystalline Systems*, Akadempriodika, Kyiv (2003) [in Ukrainian].

9. Glassy Metals: Magnetic, Chemical and Structural Properties, ed. by R.Hasegawa, CRC Press, Boca Raton, FL (1983).
10. Glassy Metals I, ed. by H.-J.Guntherodt and H.Beck, Mir, Moscow (1983) [in Russian].
11. M.von Heinmendahl, G.Kuglstatter, *J. Mat. Sci.*, **16**, 2405 (1981).
12. M.G.Scott, *J. Mat. Sci.*, **13**, 291 (1978).

Кристалізація швидкозагартованих стрічок на основі $\text{Fe}_{82}\text{Si}_2\text{B}_{16}$ при ізотермічних відпалах

О.П.Брудько, В.К.Носенко, М.І.Захаренко, Ю.П.Склярів

Магнітометричним методом досліджено кінетику кристалізації аморфних сплавів на основі $\text{Fe}_{82}\text{Si}_2\text{B}_{16}$ в процесі їх ізотермічних відпалів. Визначені енергія активації кристалізації E_a і показник Аврамі n . Показано, що добавки Ni і Mo слабо впливають на значення E_a і n . Енергія активації кристалізації для стрічок, виготовлених з використанням промислових лігатур, в межах похибки експерименту співпадає з відповідним значенням для сплавів того ж складу, виготовлених з хімічно чистих компонентів. Встановлено також, що величина n залежить, головним чином, від складу аморфного сплаву, а не від товщини швидкозагартованої стрічки.